

AD-A146 551

HIGH-SPEED MODULATION OF GAINASP LASERS(U)

1/1

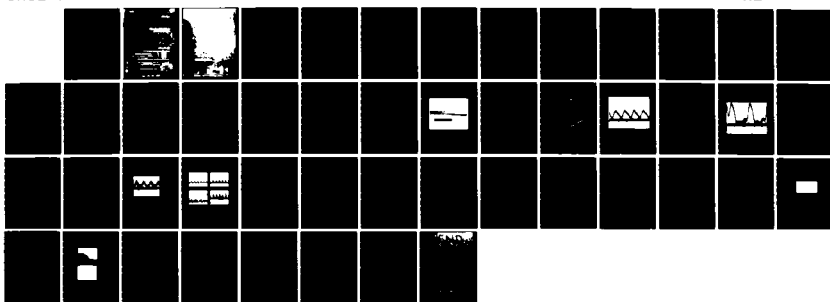
MASSACHUSETTS INST OF TECH LEXINGTON LINCOLN LAB

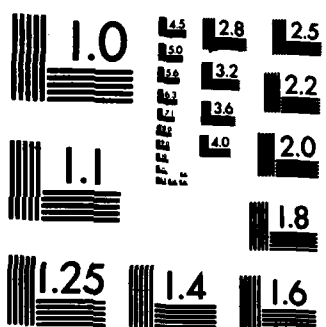
F J LEONBERGER 30 SEP 82 ESD-TR-84-027 F19628-88-C-0002

F/G 20/5

NL

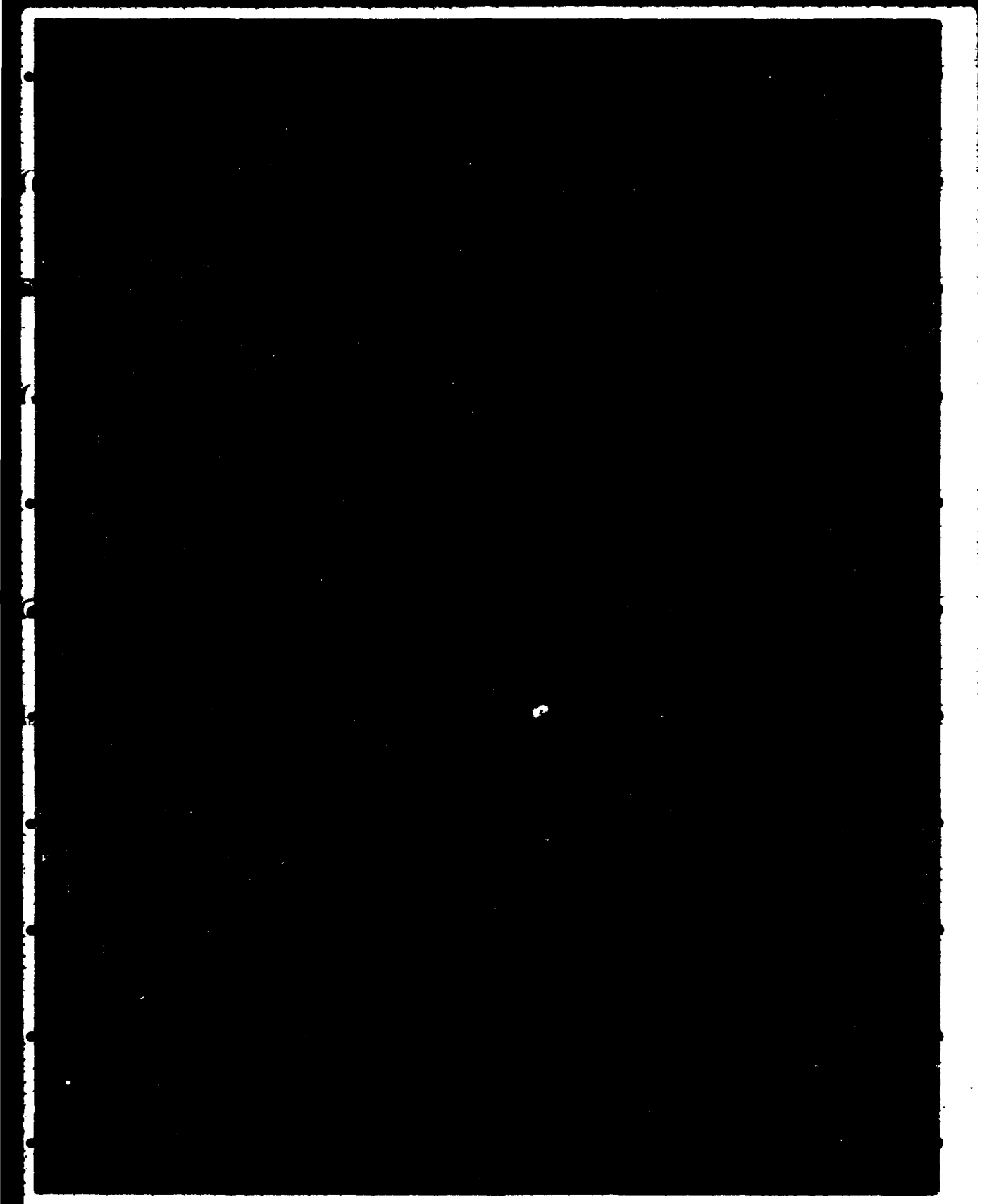
UNCLASSIFIED





OPY RESOLUTION TEST CHART

AD-A146 551



**MASSACHUSETTS INSTITUTE OF TECHNOLOGY
LINCOLN LABORATORY**

**HIGH-SPEED MODULATION
OF GaInAsP LASERS**

**FINAL REPORT
TO THE
DEFENSE ADVANCED RESEARCH PROJECTS AGENCY**

1 APRIL 1981 — 30 SEPTEMBER 1982

ISSUED 7 AUGUST 1984

Approved for public release; distribution unlimited.

LEXINGTON

MASSACHUSETTS

HIGH-SPEED MODULATION OF GaInAsP LASERS

H(+)

ABSTRACT

Q-switched diode lasers and external modulators have been developed for modulation of diode lasers at multigigahertz rates, beyond the capability of conventional current modulation techniques. Three types of Q-switched lasers were made including an H⁺-isolated buried-heterostructure (BH) version with a threshold of 40 mA and a Be-implanted BH version with a threshold of 15 mA. The lasers have a drive capacitance of well under a picofarad. The BH lasers operate continuously at room temperature. Rates as high as 7 GHz have been achieved. Simulations show the device should work at data rates of 10 Gbit/sec and higher with a binary pulse position modulation format. Several types of single-mode InP and GaInAsP waveguides, three-guide couplers and phase modulators were fabricated as initial steps in the development of multigigahertz analog modulators which could be monolithically integrated with diode lasers. Device characteristics include single-mode guide propagation loss of 1.5 cm⁻¹ at 1.15 μ m, 6-mm coupling length and a 20-V π -radian phase shift.

Accession For	
NTIS GRA&I	<input checked="" type="checkbox"/>
DTIC TAB	<input type="checkbox"/>
Unannounced	<input type="checkbox"/>
Justification	
By _____	
Distribution/	
Availability Codes	
Dist	Avail and/or Special
A-1	



HIGH-SPEED MODULATION of GaInAsP LASERS

I. INTRODUCTION

The bandwidth of optical fibers exceeds that of laser diodes, detectors, and electronic devices. The development of GaAs FETs, HEMTs, PBTs, heterojunction bipolar transistors, and small geometry high-speed silicon transistors promises multigigahertz bandwidth electronics. Two techniques to extend diode lasers beyond the capability of conventional direct current modulation techniques into the multigigahertz frequency range are explored in this study. The first, intracavity loss modulation or Q-switching, is useful primarily for digital transmission. The second, external modulation, has the potential for either analog or digital modulation.

With intracavity loss modulation or Q-switching, the laser is turned on and off by varying the loss within the laser cavity. In order to make a useful communication device, active electronic control of this loss is required. Prior to the start of this program, high threshold and heating problems with early prototypes of intracavity-loss-modulated lasers permitted operation only on a pulsed basis.^{1,2} In this study, techniques to improve heat dissipation and lower the amount of heat generation are explored. In the past year lasers have been fabricated with thresholds as low as 15 mA³ using a mass transport technique to form the buried heterostructure.⁴ These devices have successfully been continuously operated at room temperature. Previous to this study, the highest modulation rate of Q-switched lasers was 2.5 GHz. Recently, modulation has been seen to 7 GHz with full on/off modulation confirmed to at least 4 GHz. The modulators have a capacitance as low as 0.1 pF and require only a few volts of drive. Since these devices do not require the high currents required of direct current modulation, they can be easily driven when integrated with low-power transistors. The important issue of whether data (nonrepetitive signals) can be

transmitted at rates of 10 GBit/s with these devices was also explored theoretically. While the pattern of the modulation appears to preclude pulse code modulation (PCM), binary pulse position modulation (PPM) appears to be a promising technique at rates of 10 GBit/s and higher.

With external modulation, the laser is constantly on. The laser can be amplitude modulated through control of the loss in an external modulator. These modulators can potentially be applied to either analog or digital modulation formats. External modulators eliminate the complexities of the internal dynamics of the laser including frequency spreading effects at a cost of laser-to-modulator coupling problems and potentially greater optical loss than an intracavity loss structure.

In this report, we will begin with the basic concepts and theory of the Q-switched device including computer simulations of data transmission. We then explore device results based on three different structures. The first, a laser with a zinc-diffused stripe amplifier and a Be-implanted modulator had thresholds as low as 240 mA and was modulated up to 6 GHz. The second, a buried heterostructure (BH) laser with an H⁺-isolated modulator had a threshold of 40 mA and was continuously modulated at 3 GHz with full on/off modulation. With an improved detector and different instrumentation, the third device, a BH laser with a Be-implanted modulator, had a threshold as low as 15 mA and was continuously modulated to 7 GHz.

Results for the modulators are contained at the end of this report. Two types of external modulators were explored, an electroabsorption modulator and a Mach-Zehnder interferometric modulator. The linear range of the electroabsorption modulator was theoretically found to be limited although increases to as much as 50% of full transmission are possible with a pin heterostructure.

Several types of single-mode waveguides, three-guide couplers and a phase modulator were successfully fabricated and tested as initial sets in the development of wideband modulators.

II. BASIC CONCEPTS AND THEORY OF INTRACAVITY LOSS MODULATION

A. Modes of Q-switched Operation

Intracavity loss modulation is a technique that has been used to Q-switch many gas and solid-state laser systems. In those systems, it has produced high-peak-power or high-repetition-rate pulses. With increasing interest in high-bit-rate optical fiber communication systems and optical signal processing, intracavity loss modulation of diode lasers is likely to be important because of its potential for producing short pulses at high rates with essentially 100% depth of modulation.

In order to produce Q-switched operation of a laser, the switching time of loss in the laser cavity must be less than the spontaneous recombination time. For diode lasers, this requirement can be satisfied with a monolithically integrated, high-speed electroabsorption modulator as shown in Fig. 1.² This type of modulator was incorporated in two of the structures studied. Under operation, the amplifier section of this device is forward-biased to produce gain. The modulator can be reverse-biased to produce loss. The operation of the modulator is based on the Franz-Keldysh (electroabsorption) effect, i.e. the increase in optical absorption with electric field for photon energies slightly below the energy gap of the semiconductor. Measurements of this effect in GaInAsP have shown that large changes in the optical absorption coefficient can be produced by application of an appropriate electric field.⁵ For photon energies as much as 60 meV below the energy gap, the absorption coefficient can be increased from expected values of about 20 cm^{-1} to values of the order of

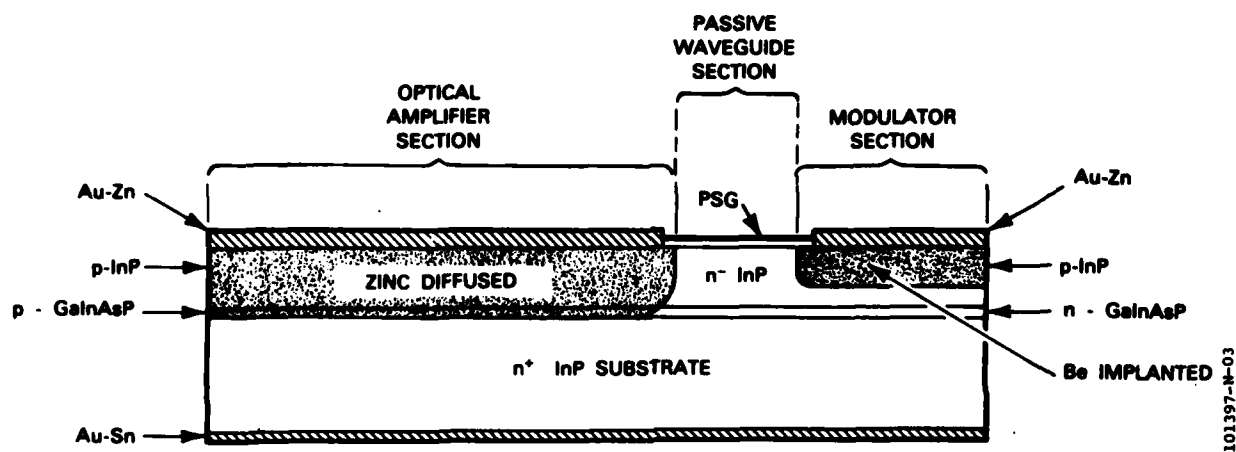


Figure 1. Schematic drawing of the laser cross section. The optical amplifier and modulator range in length from 150 to 200 μm and 50 to 75 μm , respectively. The waveguide is 25 μm long. A mesa (not pictured) is etched to provide lateral optical confinement. The endface mirrors are formed by cleaving.

1000 cm^{-1} by applying an electric field $\geq 3.6 \times 10^5 \text{ V/cm}$. Another technique would be to gain switch a short pn junction modulator, a technique which rapidly switches loss to gain. This type of modulator was incorporated in one of the structures studied. While both techniques rapidly switch loss, for simplicity only the laser with the electroabsorption modulator was analyzed.

The laser with an intracavity modulator can be analyzed with a rate equation approximation which describes the dynamics of the electron and photon populations based on considerations involving optical energy and the number of electrons. Previous theoretical treatments of actively Q-switched diode lasers have been modifications of the conventional rate equations in which the gain and loss are evenly distributed over the cavity.^{6,7} In order to include the effects of high gain and amplified spontaneous emission, a new treatment based on a rate equation approximation has been developed² to describe this device when the gain is large and when the effects of amplified spontaneous emission are important. This model, which averages spatial variations in the electron population, requires the solution of three nonlinear coupled difference equations. The numerical solution of these equations yields computer simulations of the time dependence of the spatially averaged electron population for a variety of modulation conditions. Several internal parameters for the laser device are necessary to solve these equations as discussed elsewhere.² These parameters include the spontaneous lifetime τ_{sp} , the low-loss absorption in the modulator α_L , the high-loss absorption in the modulator α_H , and the spontaneous emission factor C .

With the modulator driven at 1.65 times the threshold of the laser when the modulator loss is low, the simulations predict 20-psec pulses at 2 GHz, as shown in Fig. 2. In this mode of operation the carrier density fluctuates above

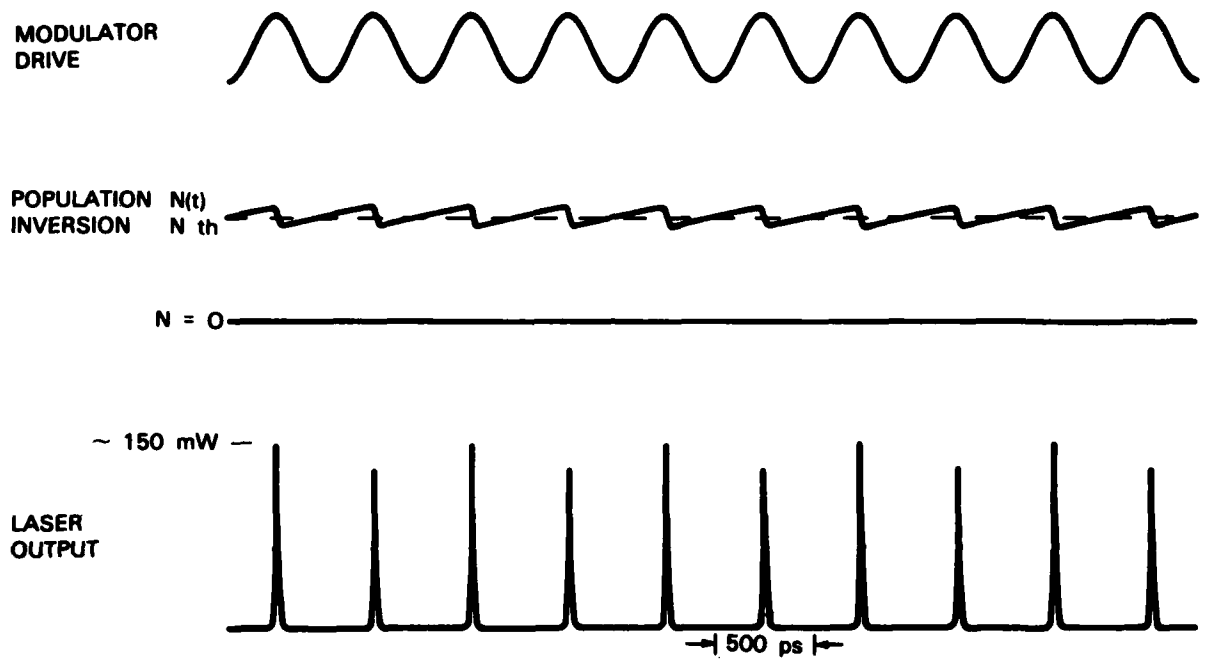


Figure 2. Inversion-dumped Q-switching calculated for a modulation frequency of 2 GHz, $I = 1.65 I_{th}$, $\tau_{SP} = 1.5$ ns, $\alpha^L = 50$ cm $^{-1}$, $\alpha^H = 350$ cm $^{-1}$, $C = 10^{-5}$, a 180- μ m amplifier, and a 70- μ m modulator.

and below its low-loss threshold value (i.e. the electron population required to produce lasing when the modulator loss is small). This mode of Q-switching will be referred to as inversion-dumped Q-switching because the inversion drops below the low-loss threshold value. At higher repetition rates, of the order of ten gigahertz, the electron population always remains above its low-loss threshold value, as shown in Fig. 3, for a modulation frequency of 10 GHz. The buildup time for the injected carrier density to reach threshold is eliminated under this high repetition rate Q-switched mode of operation. Since the electron population continuously remains at a high level above threshold, the term continuous-inversion Q-switching is used to describe this mode of operation. Among the important predictions of the model is that the buildup time of the photons from the amplified spontaneous emission is very rapid because of the high gain available in the device.

B. Predicted Digital Modulation

The possibility of transmitting digital information for applications in an optical fiber communication system at rates of 10 Gbit/s has been simulated using the rate equation treatment discussed above. Two modulation techniques, return-to-zero pulse code modulation (RZ PCM), and binary pulse position modulation (PPM), were studied. At these high bit rates, the electronic drive signals in the presence of dispersive reactances were assumed to be bandlimited as shown in the figures below. A simulation bit sequence was generated by a pseudorandom generator and plots were obtained after transients due to the initial turn-on of the laser had settled.

A representative simulation of PCM at a rate of 10 Gbit/s, with a laser pumped at 1.5 times the threshold of the device with the modulator open-circuited, is shown in Fig. 4 using parameters considered typical of the experimental devices.² The interval between the time markers is one bit

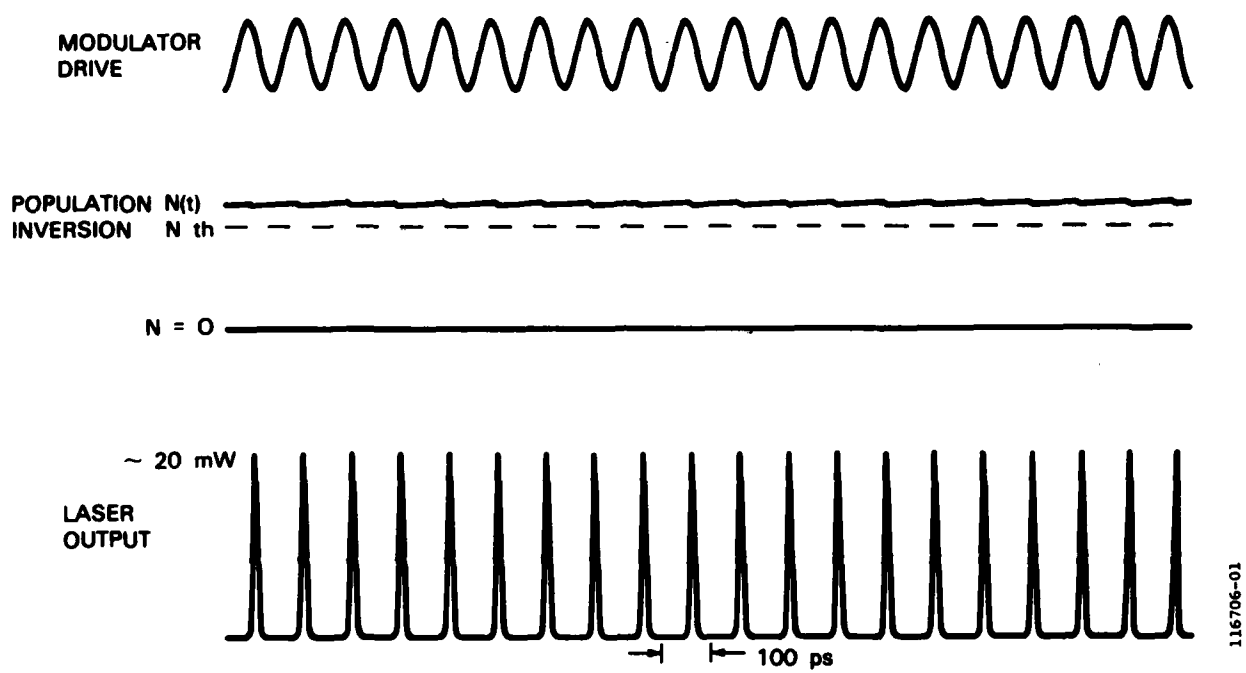


Figure 3. Continuous-inversion Q-switching at 10 GHz for $I = 1.65 I_{th}$, $\tau_{SP} = 1.5$ ns, $\alpha^L = 50 \text{ cm}^{-1}$, $\alpha^H = 350 \text{ cm}^{-1}$, $C = 10^{-5}$, a 180- μm amplifier, and a 70- μm modulator.

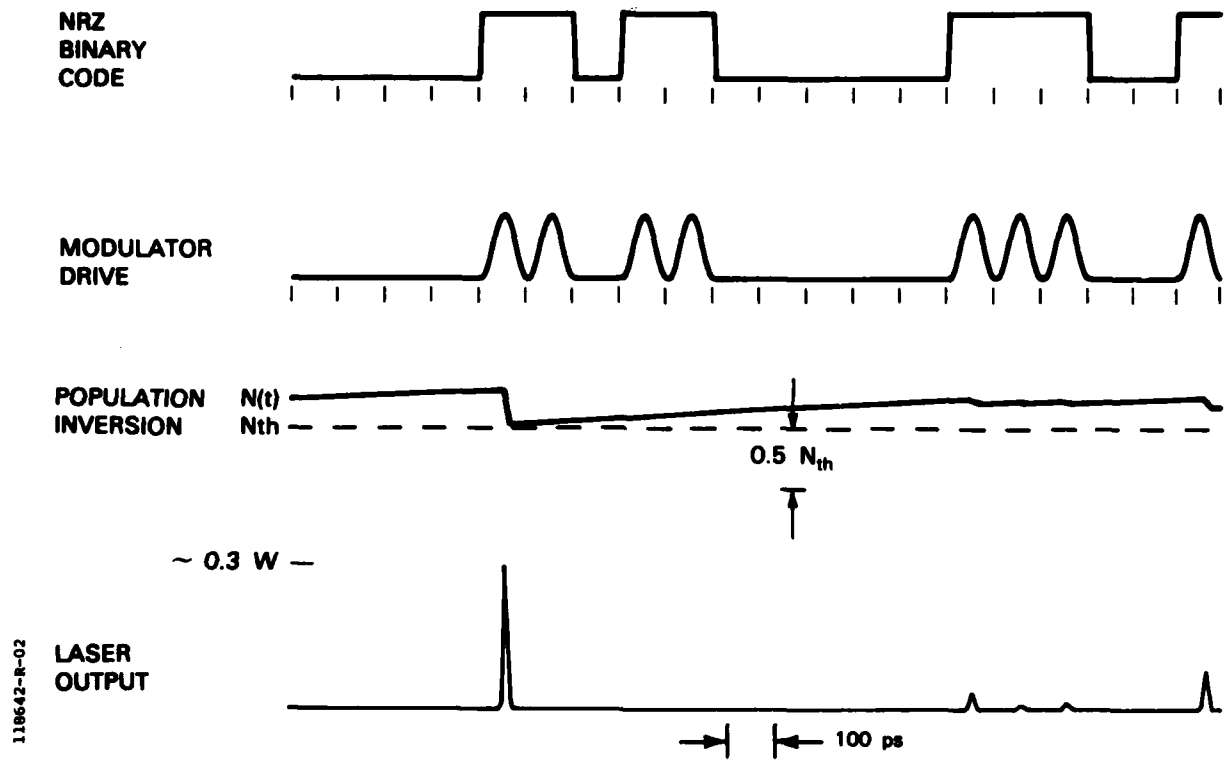


Figure 4. Simulated return-to-zero pulse code modulation at 10 Gbits/s for $I = 1.5 I_{th}$, $\tau_{sp} = 1.5$ ns, $\alpha^L = 50 \text{ cm}^{-1}$, $\alpha^H = 550 \text{ cm}^{-1}$, a 180- μm amplifier, and a 70- μm modulator. The fraction of spontaneous emission into the laser mode is assumed to be 10^{-5} . With dc reverse bias, the loss is lowest at the peaks of the modulator drive.

period. Since the modulator is reverse-biased, a positive modulator drive pulse will decrease the loss and an optical pulse should result. It can be seen that the laser is not able to respond at the modulation rate because the electron population cannot consistently return to the level required to produce laser oscillation. The problem is particularly prominent for strings of zeroes followed by strings of ones.

PPM allows the laser to maintain a more constant level of electron population since the laser is required to pulse once every bit period. Maintaining the electron population constantly above threshold is especially important for the proposed continuous inversion form of Q-switching. The duration of the modulator pulse in the presence of dispersion is adjusted for half the bit period. The model suggests that conditions suitable for binary PPM exist, as shown in Fig. 5 at a rate of 10 Gbit/sec, with the same conditions used in Fig. 4. The laser can be seen to respond with a pulse when the modulator loss is lowered. Pulse height variations due to pattern effects are evident. The peak optical power is estimated to be on the order of 10 mW for the smallest pulse however. For digital applications, the threshold can be set appropriately and the pattern effects should not prove to be a problem. The electron population, as shown in Fig. 5, is continuously above threshold and the device is operating in a continuous inversion mode of Q-switching.

III. DEVICE RESULTS

Three implementations of the Q-switched lasers were studied. We begin with the original prototype, a laser with a zinc-diffused stripe amplifier and a Be-implanted modulator. We then describe low threshold versions of the device. A buried-heterostructure (BH) laser with an H^+ -isolated modulator which is forward-biased has a modulator that operates based on a combination of gain and

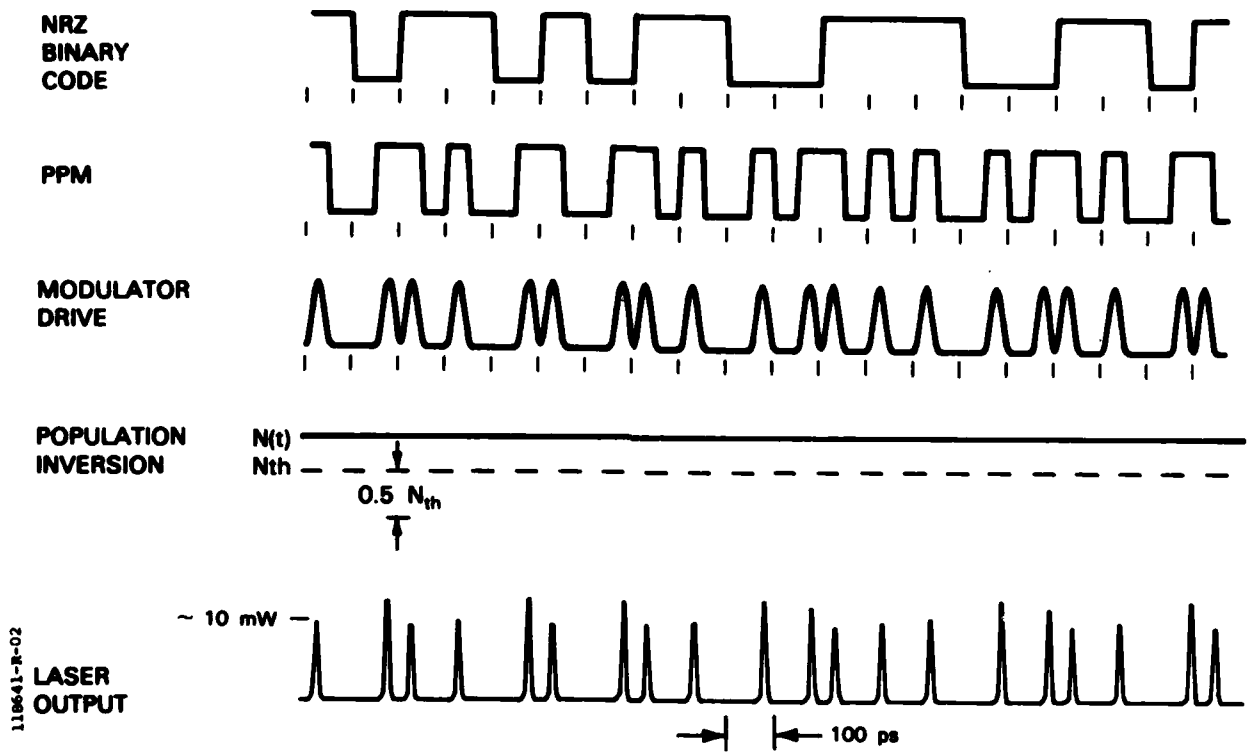


Figure 5. Simulated binary pulse position modulation at 10 Gbits/s. With dc reverse bias, the loss is lowest at the peaks of the modulator drive.
 $I = 1.5 I_{th}$, $\tau^{SP} = 1.5 \text{ ns}$, $\alpha^L = 50 \text{ cm}^{-1}$, $\alpha^H = 550 \text{ cm}^{-1}$, $C = 10^{-5}$, a 180- μm amplifier, and a 70- μm modulator have been assumed.

loss switching. The second low-threshold version is a BH version of the original device with a Be-implanted electroabsorption modulator.

A. Q-switched Laser with a Zn-diffused Stripe Amplifier and a Be-implanted Modulator

The first structure we have used to achieve active Q-switching is shown in Fig. 6. It consists of three regions: an optical amplifier section, a passive waveguide section, and an electroabsorption modulator section. The device has been fabricated in the GaInAsP-InP material system. The device structure was grown by liquid phase epitaxy (LPE) on a (100)-oriented InP (Sn) substrate doped to $2 \times 10^{18} \text{ cm}^{-3}$. A buffer layer of $2 \times 10^{18} \text{ cm}^{-3}$ n-type InP was usually grown. The step-cooling technique was used to grow a 0.2- μm -thick active layer of $\text{Ga}_{0.26}\text{In}_{0.74}\text{As}_{0.60}\text{P}_{0.40}$ and a 2- μm -thick InP cap layer. The net donor concentration in both layers was $\sim 1 \times 10^{16} \text{ cm}^{-3}$ to maintain small modulator capacitance.

Zinc was diffused through a window 10-12 μm wide in a PSG mask to form the pn junction for the amplifier section. A modulator section approximately 25 μm wide and 50 μm long was formed by selective implantation of Be ions into the InP cap, followed by annealing at 700°C for 10 min with a PSG cap layer in a flowing atmosphere of PH_3 and N_2 . The InP and GaInAsP epitaxial layers were masked and etched to leave a mesa 25 μm wide for lateral optical confinement in the waveguide and modulator sections. Plated Au-Zn contacts were microalloyed to the Zn-diffused and Be-implanted regions through a PSG insulator mask layer, and plated Au-Sn contacts were microalloyed to the n^+ substrate. Ti and Au were sputtered and photolithographically defined to form contact pads on the p side.

The device was mounted in a package between two microstriplines. Laser threshold currents with the modulator open-circuited were obtained as

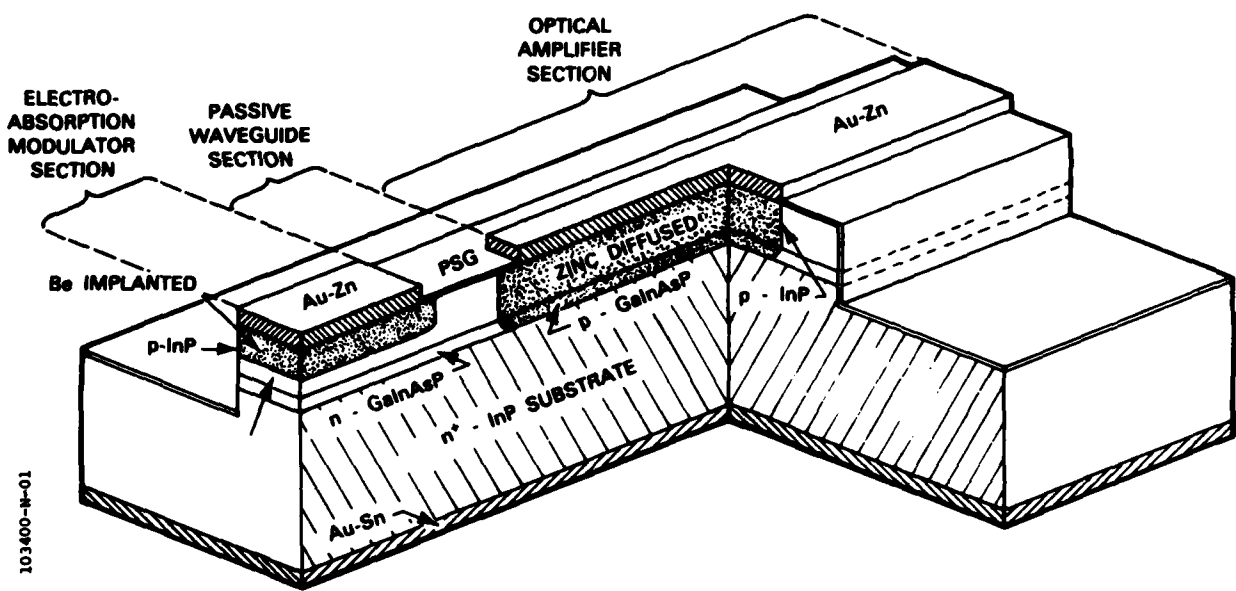


Figure 6. Schematic drawing of a Q-switched semiconductor diode laser. The device consists of a zinc-diffused amplifier section, a beryllium-implanted modulator section, and a passive waveguide section.

low as 240 mA. These lasers have been tested on a pulsed basis using the system shown in Fig. 7. A similar system is used for all the laser modulation results. With the modulator biased about a dc operating point, a microwave drive signal is applied to the modulator. The optical output is detected with a GaInAsP photodiode characterized by less than 100-ps rise and fall times. The detected signal is then displayed on a sampling oscilloscope. Figure 8 shows full on/off modulation of the laser diode at a rate of 3 GHz for a laser drive current 1.6 times the threshold current of the device with the modulator open-circuited. The dc bias on the modulator was 12 V and the microwave power was 310 mW. The oscilloscope trace has been taken near the end of the gain section excitation pulse. At the end of the laser pulse train, electrical pickup at the 3-GHz modulation frequency is evident. The full width half maximum of the output trace is about 120 ps.

Modulation at frequencies up to a measurement system limit of 6 GHz has been clearly observed. The frequency response of the measurement system is presently limited by the GaInAsP photodiode and the depth of modulation cannot be determined.

The numerical simulations indicate that these experiments, with lasers operating at the modulation frequency of 2 - 3 GHz and a current drive of 1.5 - 2.0 times threshold, can be best interpreted with the inversion-dumped mode of Q-switching for recombination lifetimes of a few nanoseconds. Significantly larger lifetimes are required in order to apply the continuous inversion interpretation.

The devices were soldered p-side down onto a beryllia heatsink which also served as a microstripline. Although 1.7 W of power was dissipated from the laser chip without destruction of the device, cw operation was not achieved. This was in part due to high electrical series resistance in the devices

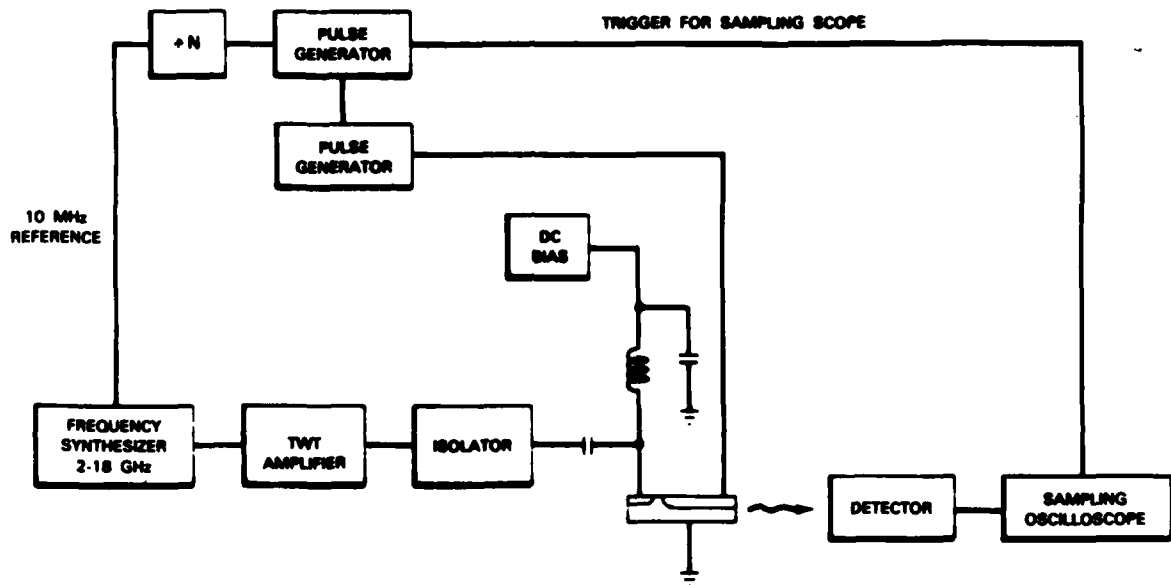
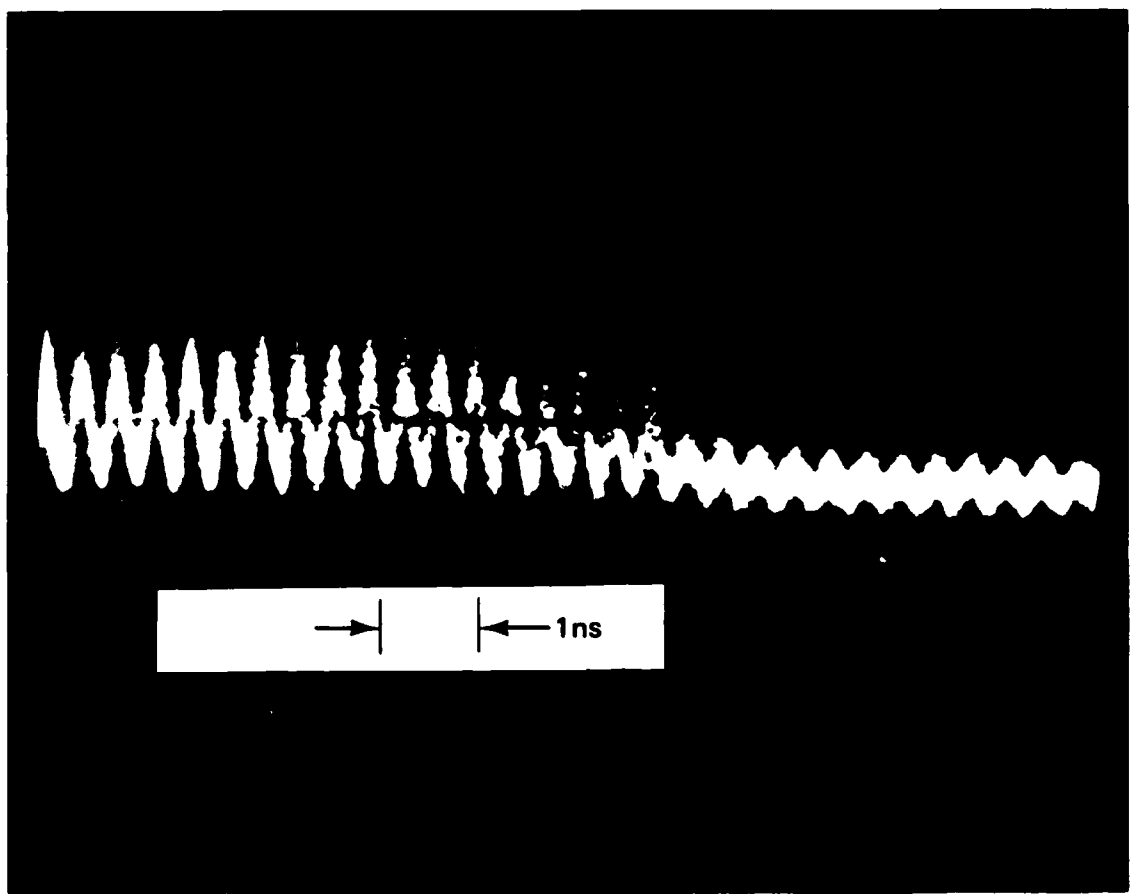


Figure 7. Block diagram of the experimental system.



141716-S

Figure 8. Pulse train from Q-switched diode laser at 3 GHz shows full on/off modulation.

available at that time. Although better heatsinking could be achieved with the stripe side of the device soldered to the heatsink, the devices were generally mounted with the substrate side down to facilitate contacting the amplifier and modulator sections.

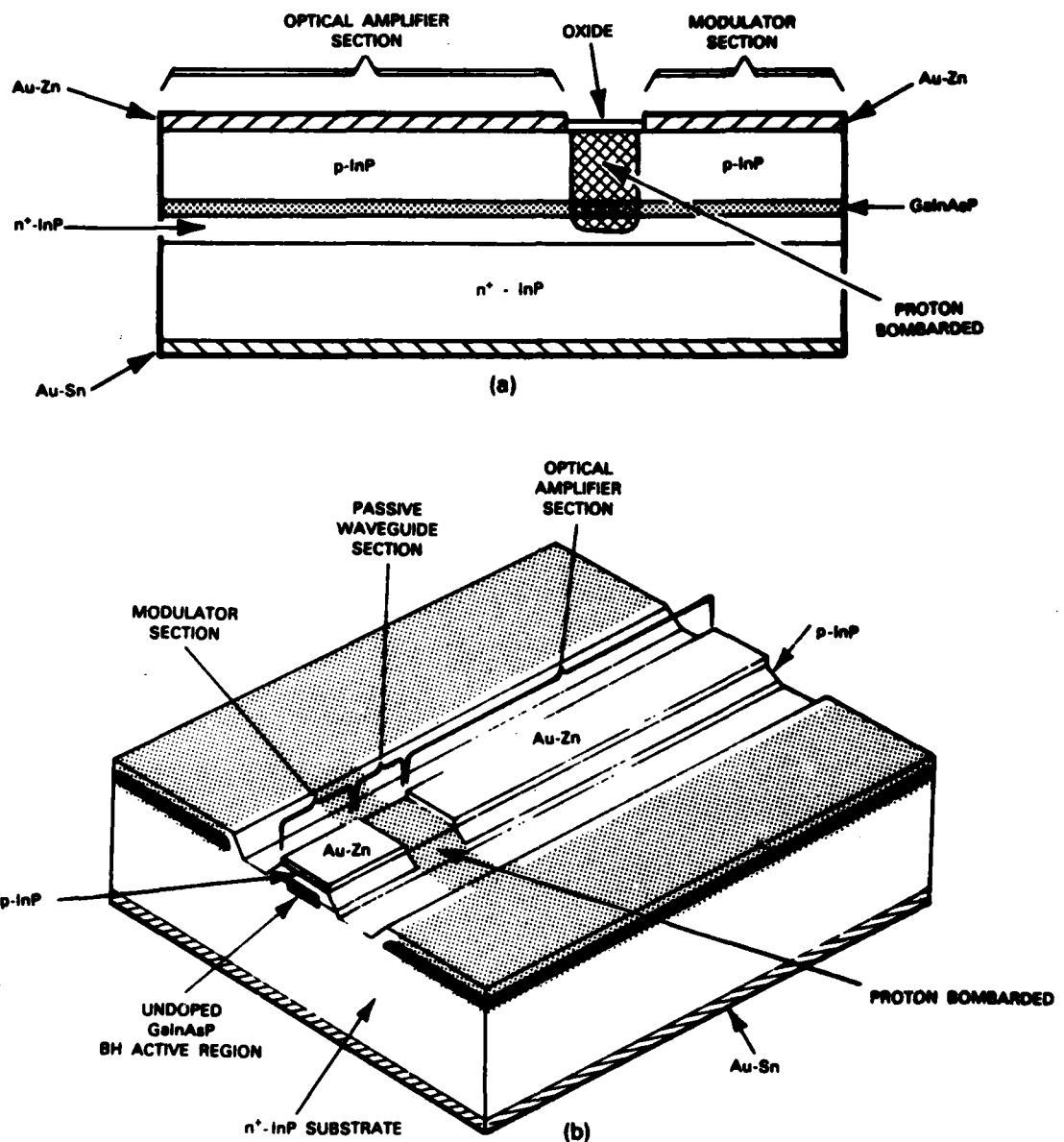
B. Buried Heterostructure Q-switched Laser with an H^+ -isolated Modulator

A cross section of the second diode laser with two electrically isolated buried heterostructure sections is shown in Fig. 9(a), while the perspective view is shown in Fig. 9(b). The device operation is based on a combination of gain switching and Q-switching in which both gain and loss are actively varied in a modulator section while an amplifier section is driven with a constant dc current.

The device was fabricated from a double heterostructure wafer consisting of a p-InP cap layer, a nominally undoped GaInAsP active region, an n⁺-InP buffer layer and an n⁺-InP substrate. The buried active region is formed by an etching and mass transport process.⁴ The wafer is proton bombarded to produce a laser with a long amplifier section ($\sim 200 \mu\text{m}$) and a short modulator section (~ 50 to $100 \mu\text{m}$) electrically isolated from each other by the high-resistivity bombarded region ($20 \mu\text{m}$).

With uniform dc current density applied to each section, the laser threshold was as low as 17 mA. With a small forward voltage < 0.8 V in the modulator, such that no significant current injection occurs, the laser threshold for current through the amplifier was over 60 mA, three times that of the uniformly pumped laser.

Full on/off modulation up to 3 GHz has been seen at a forward bias of 0.8 V with only about 10 mW of microwave power applied to the modulator and about 60 mA of dc current applied to the amplifier (Fig. 10). As the amplifier current



129017-N-01

127920-N-02

Figure 9. (a) Cross section of a Q-switched laser with a proton-isolated modulator. The proton bombarded region is high resistivity. The electrical isolation is well over a megohm, (b) perspective view of the Q-switched laser with a proton-isolated modulator shows the buried heterostructure active region and the extent of the proton-bombarded region.



Figure 10. Q-switched output at 3 GHz from the laser with proton-isolated modulator. Modulator is forward-biased and operates by both gain and loss switching.

was increased, subharmonic operation was seen at 1.5 GHz. A substantial increase in the peak signal level was noted at the subharmonic, an indication of energy storage and Q-switching as shown in Fig. 11.

Under modulation, significant forward current is injected into the modulator section to switch the loss rapidly into gain. A Q-switched pulse can then rapidly build and dump the electron population in both sections. Since the turn-on time of the modulator is limited only by its capacitance and the drive current, while the turn-off time is dependent on the stimulated lifetime, operation well above a gigahertz is possible depending on how hard the sections are driven. These low-threshold lasers are capable of producing short pulses at high rates with low microwave power requirements.

C. Buried Heterostructure Q-Switched Laser with a Be-Implanted Modulator

The buried heterostructure version of the laser with a Be-implanted modulator was fabricated from a double heterostructure wafer using both selective chemical etching and mass transport⁴ to create a buried active region about 2 μ m wide. Zinc was selectively diffused to form an amplifier section and beryllium was implanted to form a modulator section as shown in Fig. 12. The forward-biased amplifier and the reverse-biased modulator are optically coupled but electrically isolated by the waveguide section. The buried active region is shared by all three sections.

The lasers have thresholds as low as 15 mA with the modulator open-circuited. In order to characterize the device, the pulsed threshold of the laser is measured as a function of the modulator reverse bias (Fig. 13). The threshold increases by a factor of about 4.5 with a 13-V reverse bias, indicating that the modulator is very effective.

The devices are modulated by application of either a pulse or dc current to the amplifier and both a dc voltage and a microwave signal to the

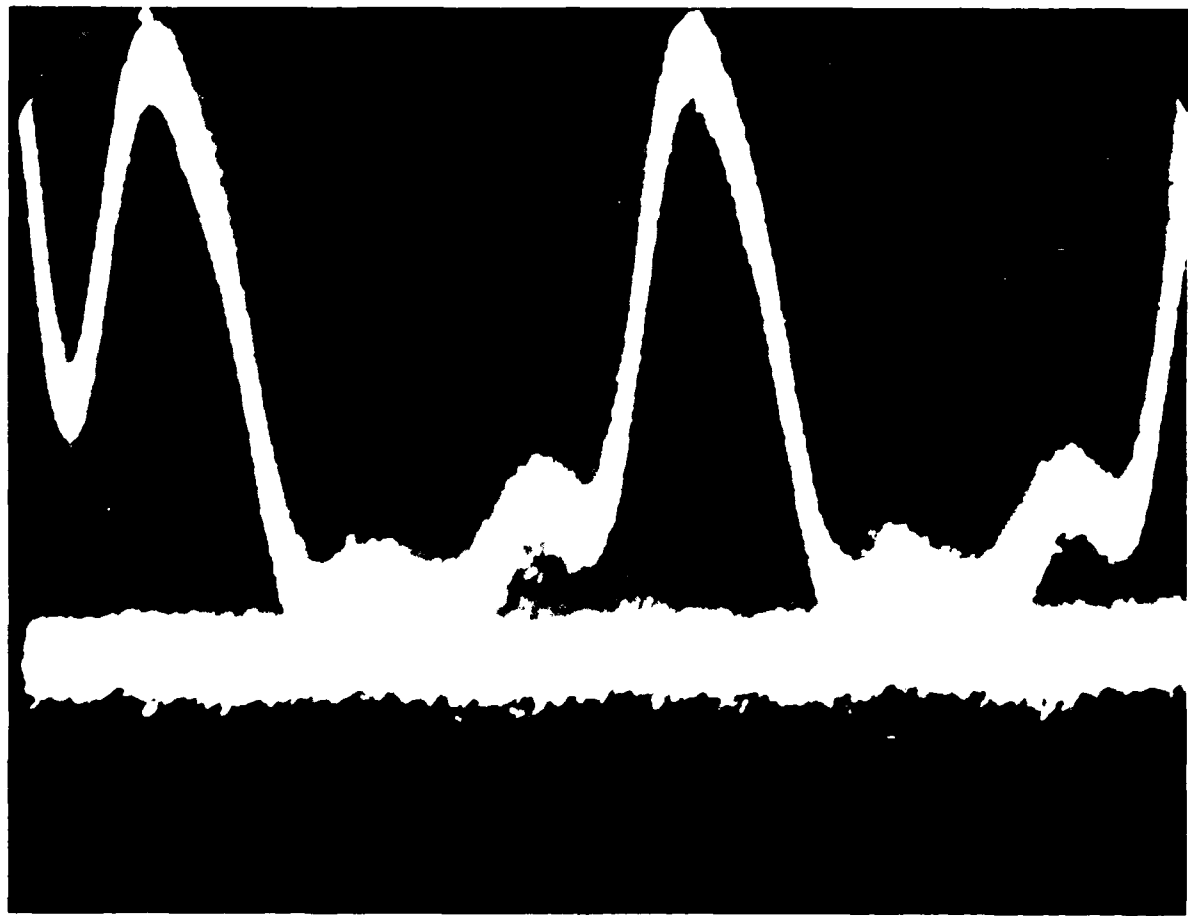
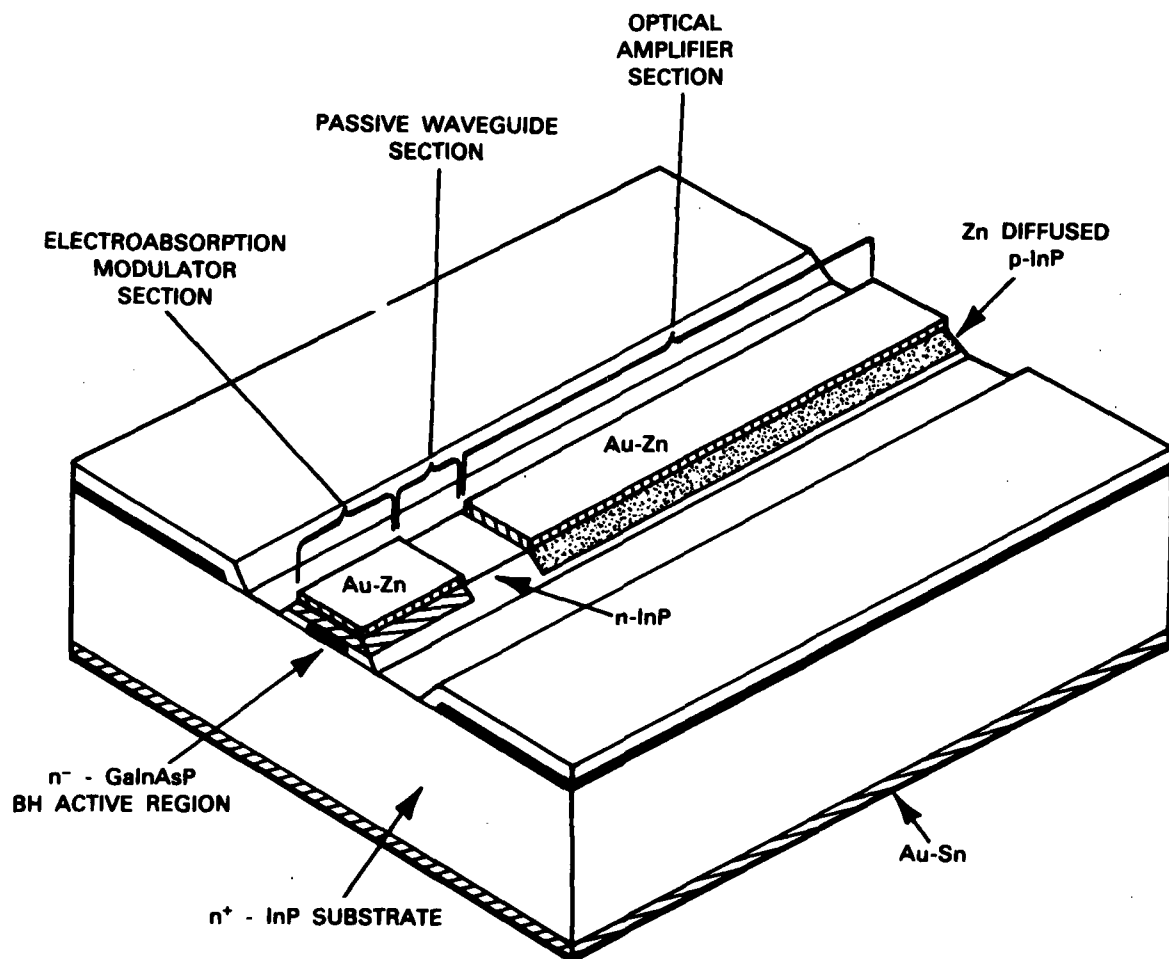


Figure 11. Subharmonic operation at 1.5 GHz with a 3-GHz modulation signal applied to the proton-isolated modulator.



127921-N-01

Figure 12. Perspective view of the Q-switched laser with a Be-implanted modulator. The 4- μ m stripe width and 50- μ m length of the modulator results in a modulator capacitance of 0.1 - 0.5 pF. The amplifier is about 200 μ m long, while the passive waveguide is about 25 μ m long.

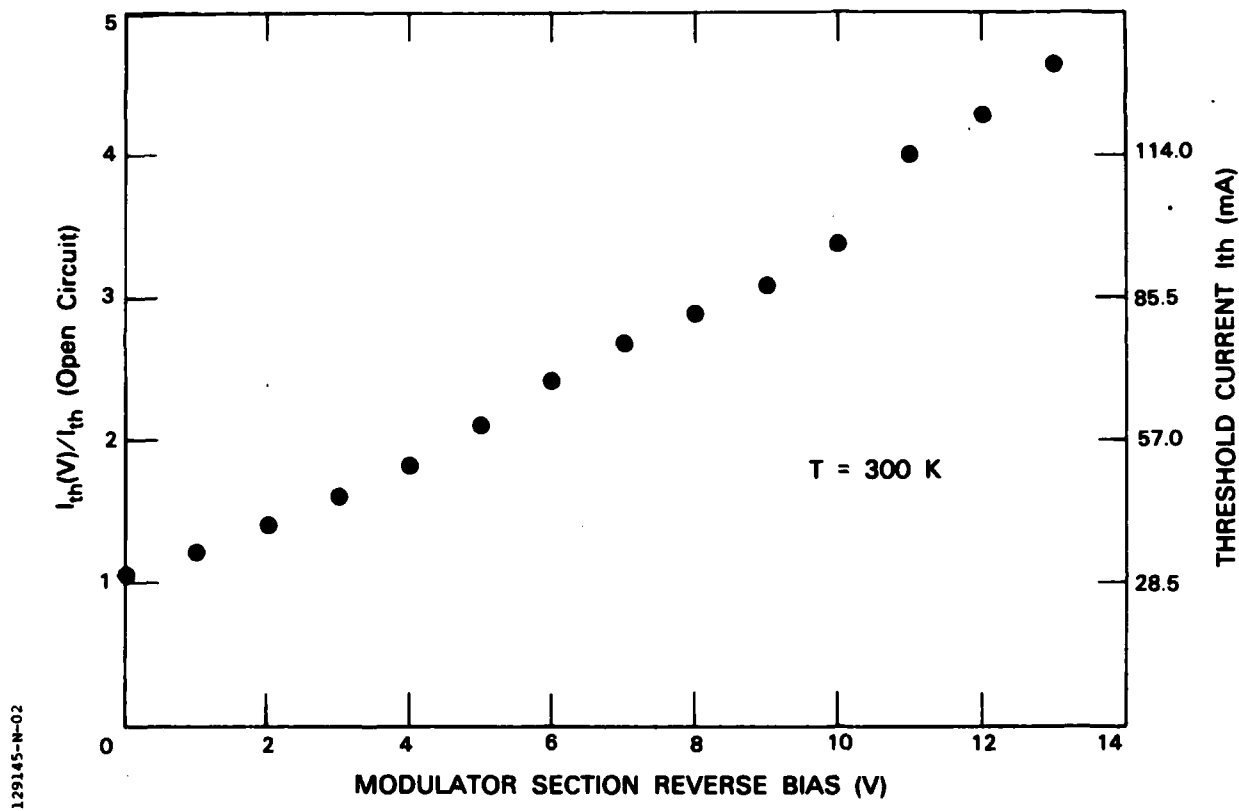


Figure 13. Pulsed threshold, normalized to the threshold of the laser with the modulator open, as a function of modulator reverse bias.

modulator. Typically 70 to 200 mW of microwave power and about 3 V of dc reverse bias are sufficient to drive the unmatched modulator. The devices Q-switch at rates between 2 and 7 GHz, as shown in Fig. 14 for a modulation rate of 4 GHz. Full on/off modulation of the laser is observable over much of this frequency range. Various types of behavior including subharmonic operation and irregular pulsations were seen when the operating conditions of the laser were varied. In particular, by increasing the amplifier current with the modulation frequency held constant, a number of operational modes were observed, consistent with theoretical predictions. At 2 GHz, when the amplifier current is just sufficient to produce laser oscillation, laser pulses are observed at the modulation frequency, as seen in Figs. 15(a) and (b). As the current is increased, the intensity of the pulses increases until a transition region in which the laser produces irregular pulsations is encountered, as seen in Fig. 15(c). With still higher current, the laser again operates at the fundamental of the modulation frequency, Fig. 15(d). Previous modeling indicates that the device operates in a continuous-inversion mode of Q-switching just above threshold in which the population inversion remains continuously high. The stimulated lifetime of an electron is long and the population does not have time to dump. The small pulse height is consistent with this explanation. The modeling also suggests that as the current increases, the laser moves into a transition region until finally inversion-dumped Q-switching, in which the population drops below threshold, is observed. In the transition region, a large pulse is sometimes emitted; however, the electron population does not have time to recover before the modulator loss again swings low and the resulting pulse is weak or omitted entirely. With higher current, the current is sufficient to rebuild the electron population each time the loss is lowered. The pulse height

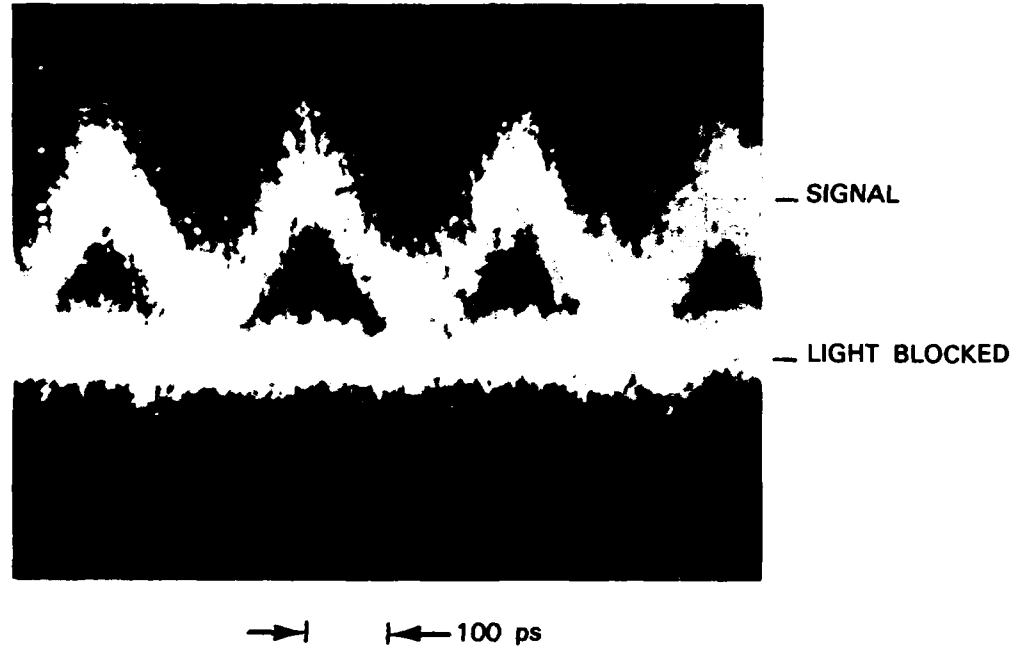
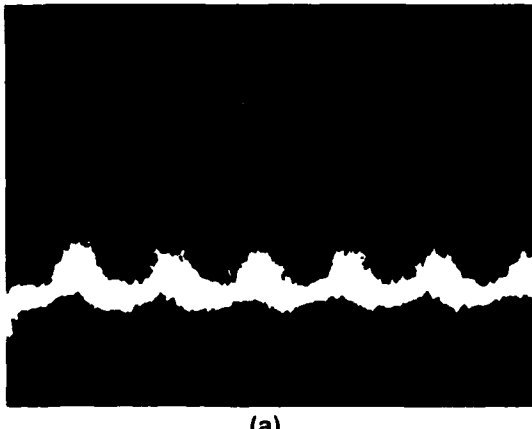
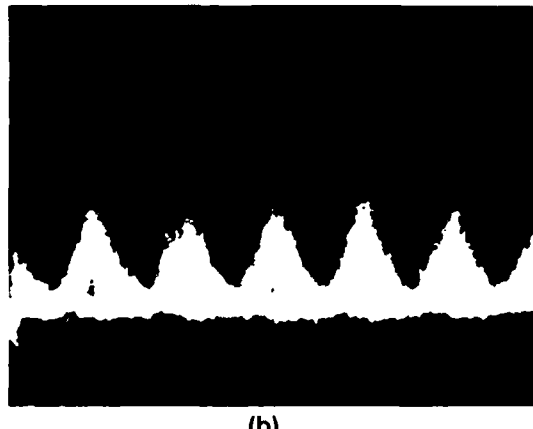


Figure 14. On/off operation of the BH laser with Be-implanted modulator at 4 GHz. One trace shows the reference obtained when the light is blocked.

CONTINUOUS INVERSION Q-SWITCHING

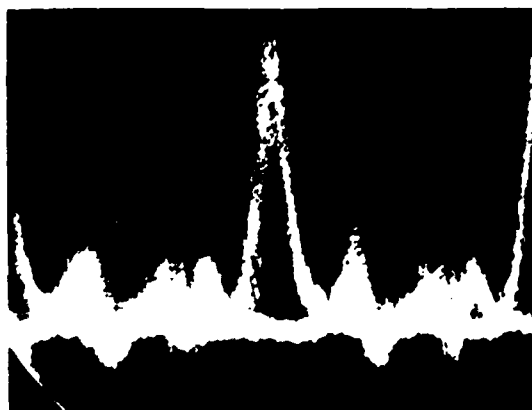


(a)



(b)

TRANSITION REGION



(c)

INVERSION-DUMPED Q-SWITCHING



(d)

129146-R-03

Figure 15. Effect of increasing the amplifier current (a) 50 mA, (b) 54 mA, (c) 59 mA, and (d) 68 mA at 2 GHz with the modulator drive held constant. The dc threshold of this laser is 30 mA with the modulator open. Figures (b)-(d) have an extra trace which shows the zero reference obtained when the light is blocked.

is consistent with inversion-dumped Q-switching. The present results provide first experimental evidence of a continuous-inversion Q-switching mechanism.

D. External Modulation

A preliminary investigation of waveguide technology to fabricate external laser modulators was also conducted in this program. The motivation is to form analog or digital waveguide modulators monolithically integrated with, but external to, the cavity of a GaInAsP diode laser. Such a structure is depicted in Fig. 16. External modulators avoid the frequency spreading and chirping effects which characterize direct-current modulation of lasers. Eliminating this frequency spread reduces the fiber dispersion effects so that longer repeater spacing can be achieved in telecommunications. Perhaps more importantly, the analog modulation capabilities provided by such modulators should allow higher bandwidth analog data transmission since nonlinear effects in direct current modulated lasers limit the useful analog bandwidth to well below the laser relaxation oscillation frequency for many applications. The calculated bandwidth of InP waveguide modulators at $1.3 \mu\text{m}$ can be $\sim 3 \text{ GHz}$ for lumped modulators and $> 10 \text{ GHz}$ for traveling-wave devices.

This work was directed towards the development of Mach-Zehnder interferometric modulators and electroasorption modulators for analog modulation. Two types of single-mode strip guides were fabricated and evaluated. These included LPE-grown GaInAsP guides on InP and InP guides formed by vapor phase lateral overgrowth of InP over SiO_2 . Three-guide couplers and phase modulators were also demonstrated. The Mach-Zehnder modulator is shown in Fig. 17 and consists of two three-guide couplers functioning as input and output beam splitters, separated by phase modulators. The three-guide couplers are used to avoid

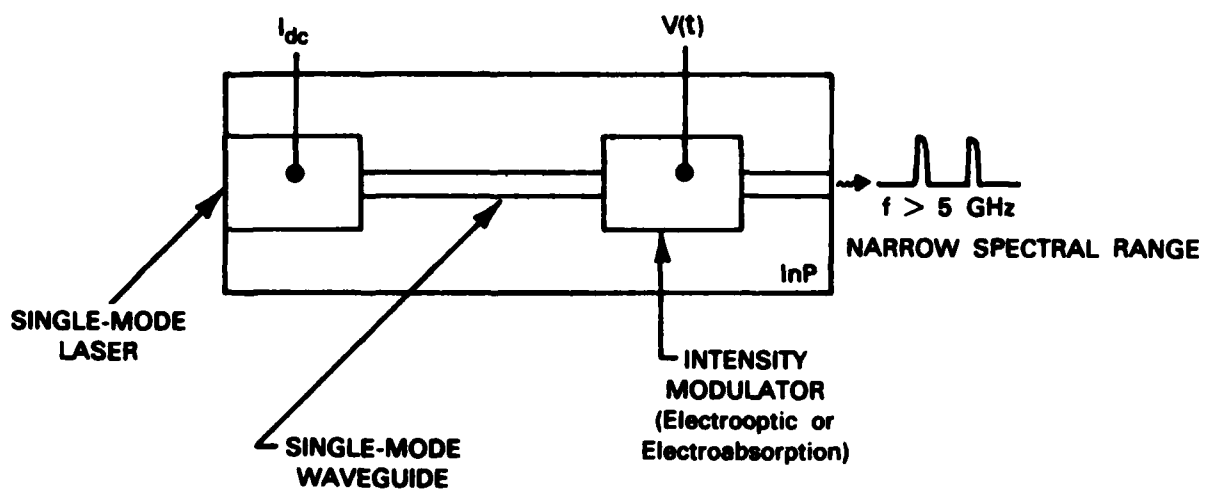


Figure 16. Schematic diagram of monolithically integrated laser and external modulator.

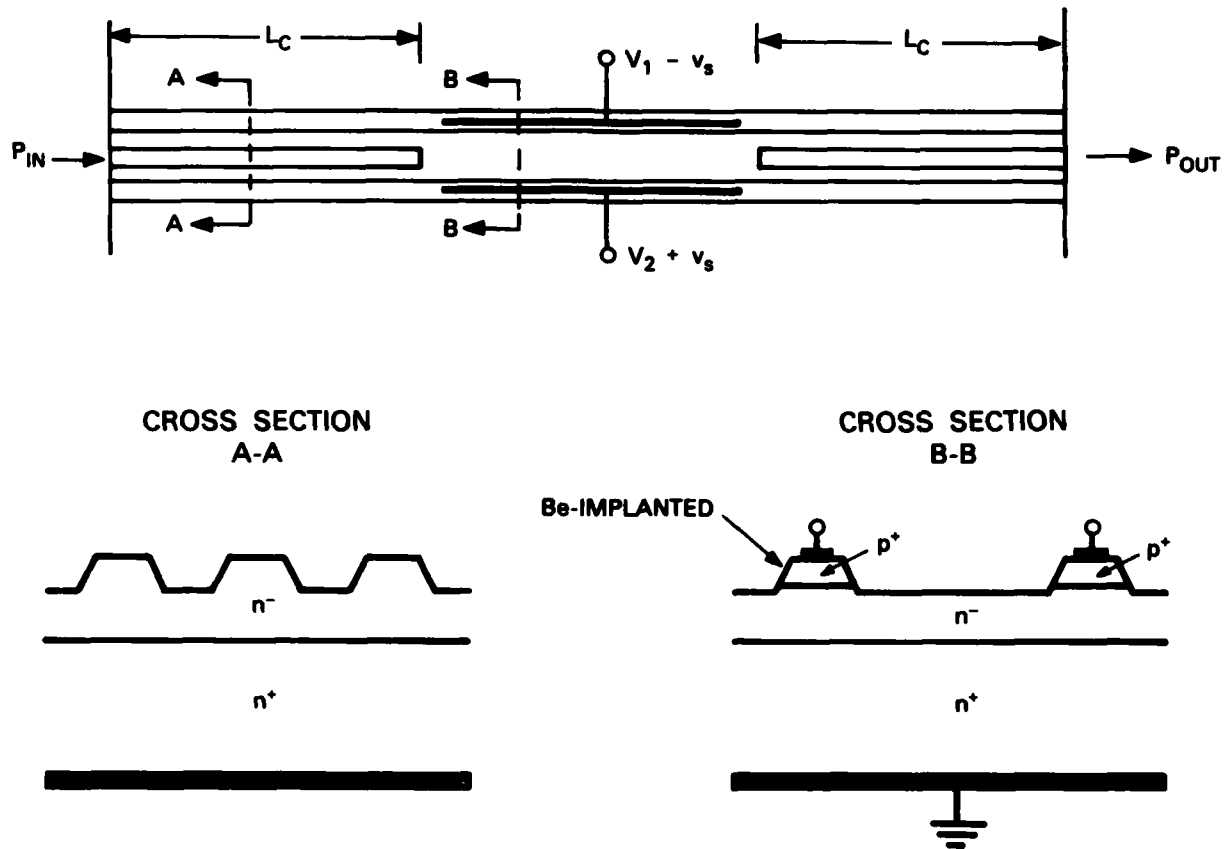


Figure 17. Schematic diagram of GaInAsP Mach-Zehnder interferometric modulator. The three-guide couplers at the input and output function as beam splitters. Modulation is achieved in the pn junction regions.

the necessity of making waveguide bends. The transfer function of this device is $P_{out} = P_{in} (1 + \cos KLV)$ where L is electrode length, V is the applied voltage and K is a constant dependent on material electrooptic properties. The device has a reasonably large linear range whose limits are set by system-acceptable distortion [$KLV(t)/\sin KLV(t)$] and detector sensitivity. The electroabsorption modulator is a p^+n waveguide structure that has a transfer function $I = I_0 e^{-\alpha L}$ where α is the electroabsorption coefficient, dependent on field and wavelength.⁸ For fields of $\sim 10^5$ V/cm, one can obtain an increase in α of 10^3 cm^{-1} . A p^+ InP/n InGaAsP/n⁺ InP waveguide structure had a limited linear range that could be increased to $\sim 50\%$ of full transmission by incorporation of a nearly intrinsic quaternary layer between the p^+ InP and the n-type quaternary layer, as illustrated in Fig. 18.

A single-mode rib waveguide structure formed in GaInAsP⁹ is shown in Fig. 19. The quaternary layers have a uniform thickness that varied between wafers in the 3- to 5- μm range. High purity material ($n = 2 - 5 \times 10^{15} \text{ cm}^{-3}$) prepared by special pregrowth baking procedures was used to minimize optical loss. The guides are ~ 3 to 6 μm wide and etched ~ 0.3 to 1 μm to achieve single-mode operation. The substrate is Fe-doped InP. To form modulators, the top part of the n-rib would be converted to p^+ to provide a junction that could be reverse-biased (see Fig. 17). To determine the propagation loss, transmission through several lengths of the same samples was measured for a number of guides using an endfire coupling technique. For GaInAsP with a band-gap corresponding to 1 μm , single-mode waveguide losses as low as 1.7 cm^{-1} at 1.3 μm and 2.7 cm^{-1} at 1.15 μm have been measured, as shown in Fig. 20. These values are comparable to single-mode LPE GaAs/GaAlAs guides.

The other waveguide structure evaluated was an oxide-confined InP guide, as illustrated in Fig. 21. This device is analogous to structures reported in

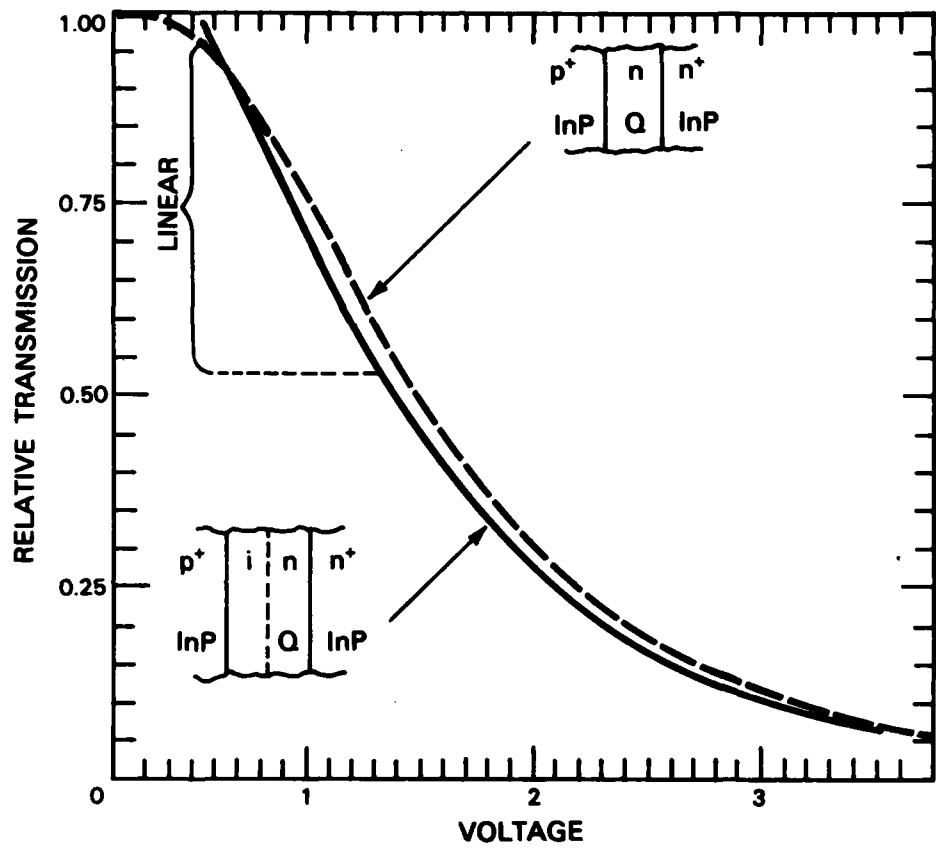
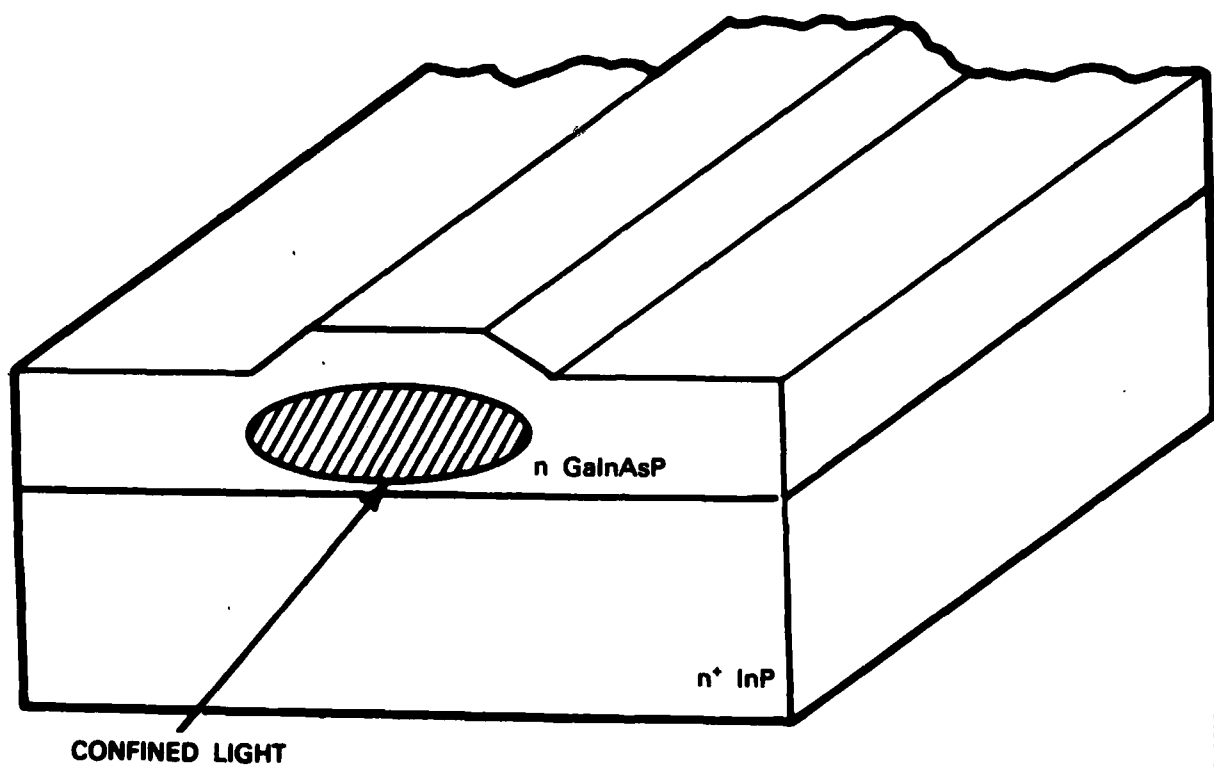


Figure 18. Transmission vs voltage for a GaInAsP electroabsorption modulator indicating the increased linear region obtained using an intermediate i-quaternary region.



141719-R

Figure 19. Schematic diagram of single-mode GaInAsP rib waveguide.

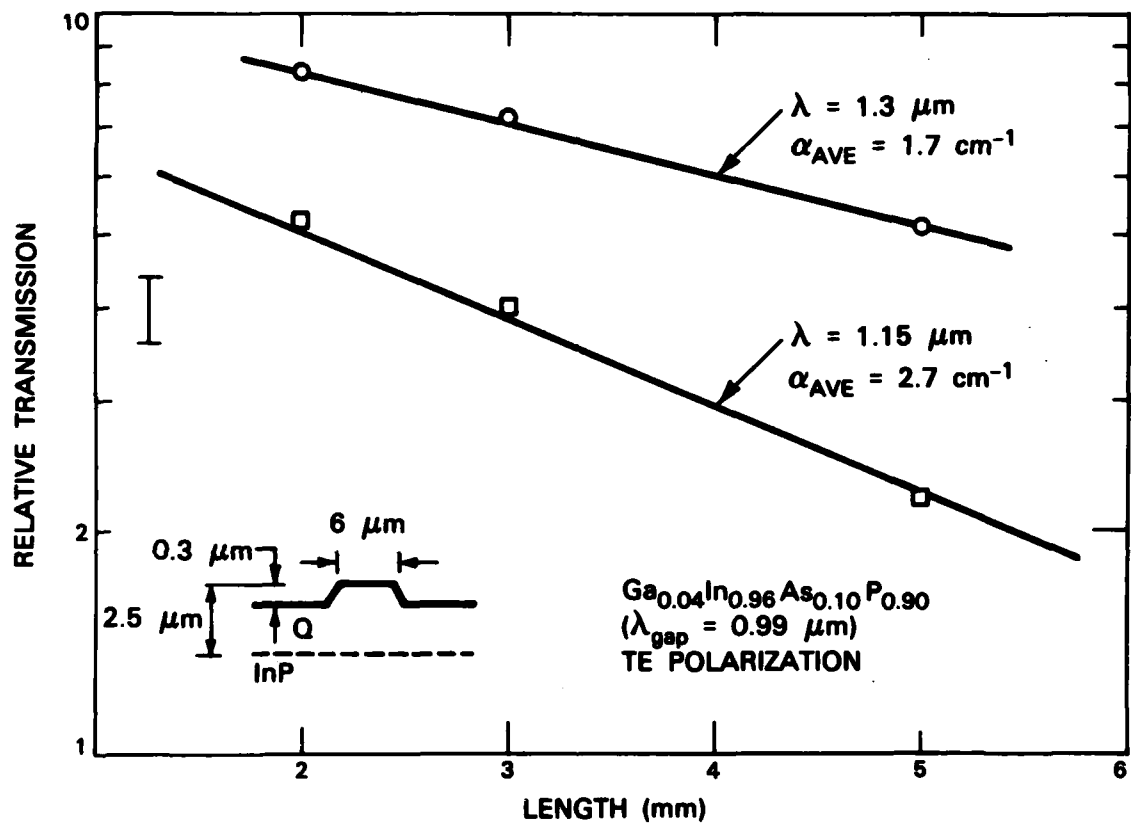


Figure 20. Transmission vs length for single-mode GaInAsP rib waveguides.

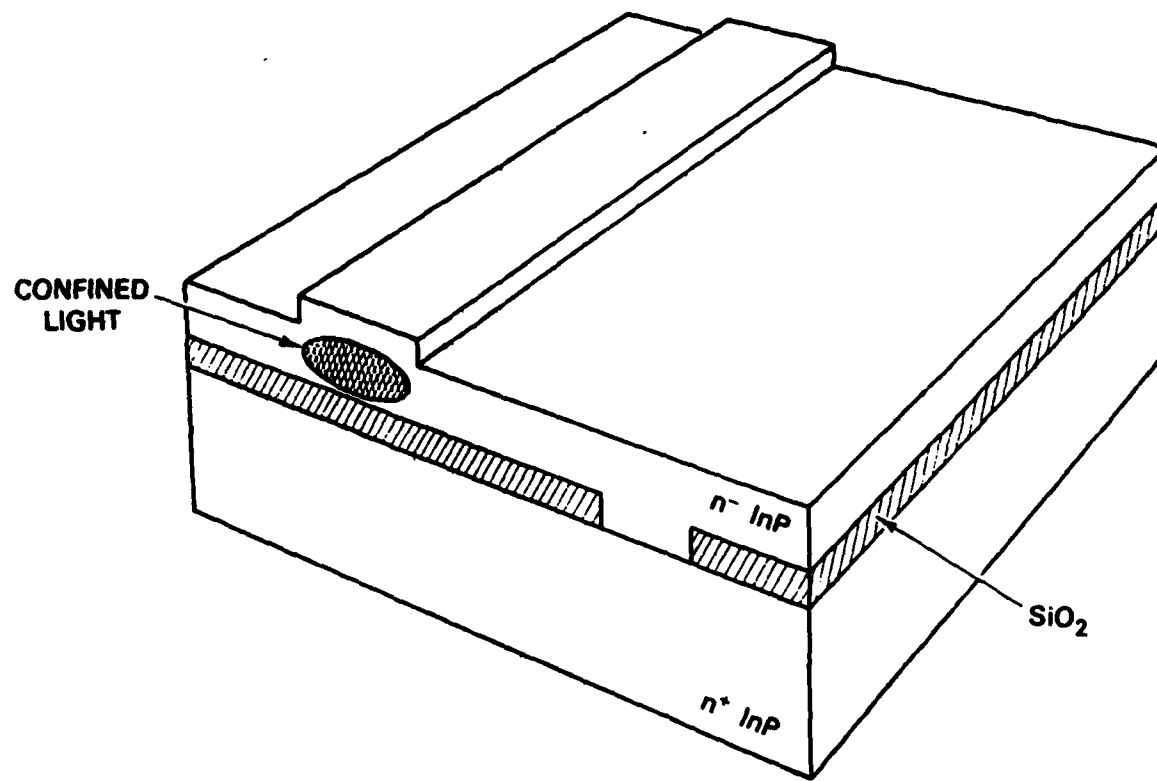


Figure 21. Schematic drawing of oxide-confined InP rib guide.

GaAs¹⁰ which have demonstrated the lowest loss for single-mode semiconductor guides (0.5 cm^{-1} or 2 dB/cm). The device is formed by nucleating PCl_3 -vapor-phase growth of InP in stripe openings in an SiO_2 film. Single-crystal growth conditions are adjusted to maximize the lateral-to-vertical rate^{11,12}.

Using this technique, a lateral-to-vertical growth rate of 3 could be obtained for stripes oriented within 10° of normal to $\langle 110 \rangle$ cleavage face. This ratio is $\sim 3X$ less than could be obtained in GaAs. For the $50\text{-}\mu\text{m}$ stripe spacing used, guides were formed but the films were not continuous for thicknesses appropriate for single-mode guide formation. It was observed that the single-crystal growth would also occur downward into etched depressions. This phenomena was exploited to form inverted rib guides as shown in the photomicrograph of Fig. 22. Here, slots were first etched in the InP substrate and then overcoated with SiO_2 . Openings in the SiO_2 films were positioned near the slots as shown.

Loss measurements were made on rib guides formed on the structure shown in Fig. 23. Here, $3\text{-}\mu\text{m}$ -wide oxide stripe openings spaced by $50 \mu\text{m}$ were oriented at $\sim 30^\circ$, the optimum angle for lateral growth, and a continuous film grown. Single-mode rib guides were formed normal to the cleavage, resulting in guides that crossed multiple stripe openings. These guides were $9\text{-}\mu\text{m}$ wide, formed on $5\text{-}\mu\text{m}$ -thick epi and etched $1 \mu\text{m}$. A loss of 1.5 cm^{-1} was obtained by measuring several lengths of the same sample at $1.15 \mu\text{m}$.

Similar structures were used to form three-guide couplers. These devices had $5\text{-}\mu\text{m}$ -wide guides separated by $5 \mu\text{m}$. The 3-dB coupling length at $1.3 \mu\text{m}$ was determined to be $\sim 6 \text{ mm}$ by measuring the relative power in the three guides for several sample lengths. A photomicrograph of the output face of a device cleaved to this length is shown in Fig. 24 along with a photograph of the near-

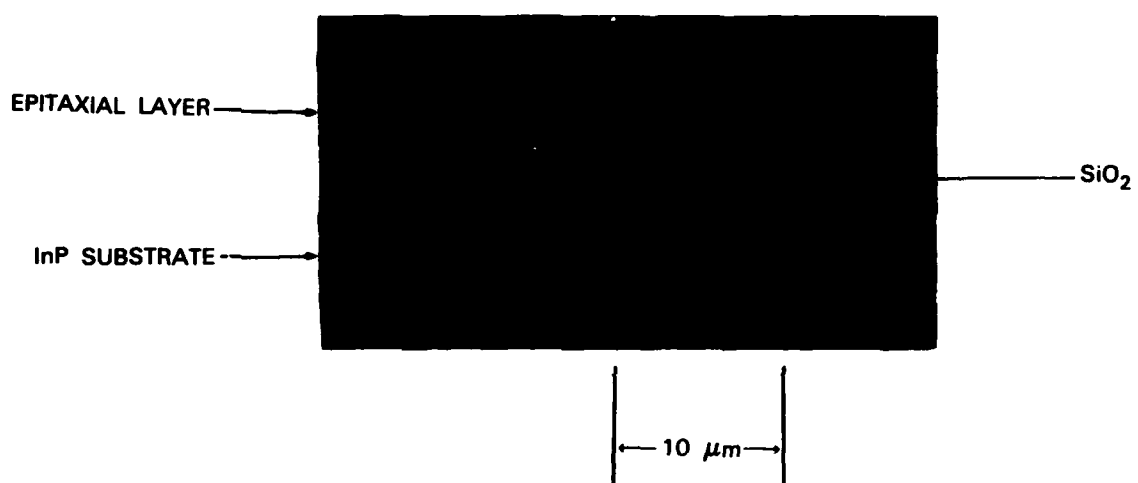


Figure 22. Photomicrograph of oxide-confined single-mode InP optical waveguide with planar inverted rib structure.

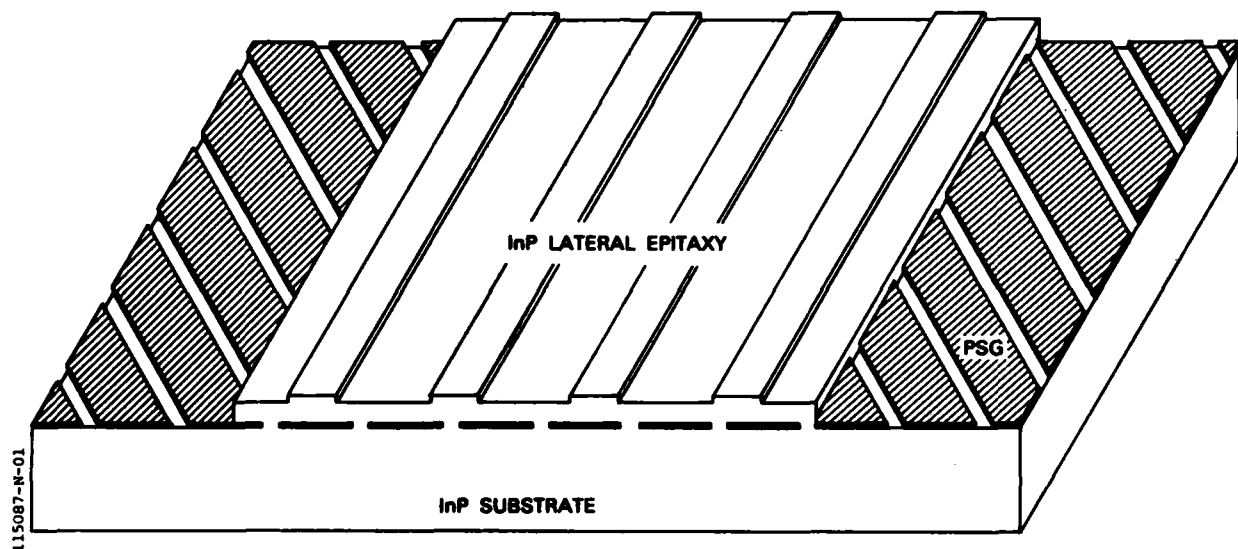


Figure 23. Schematic drawing of InP oxide-confined guides formed on wafers in which the angle of the phosphosilicate glass (PSG) stripe openings is optimized for continuous growth and the guides are oriented normal to a cleavage plane.

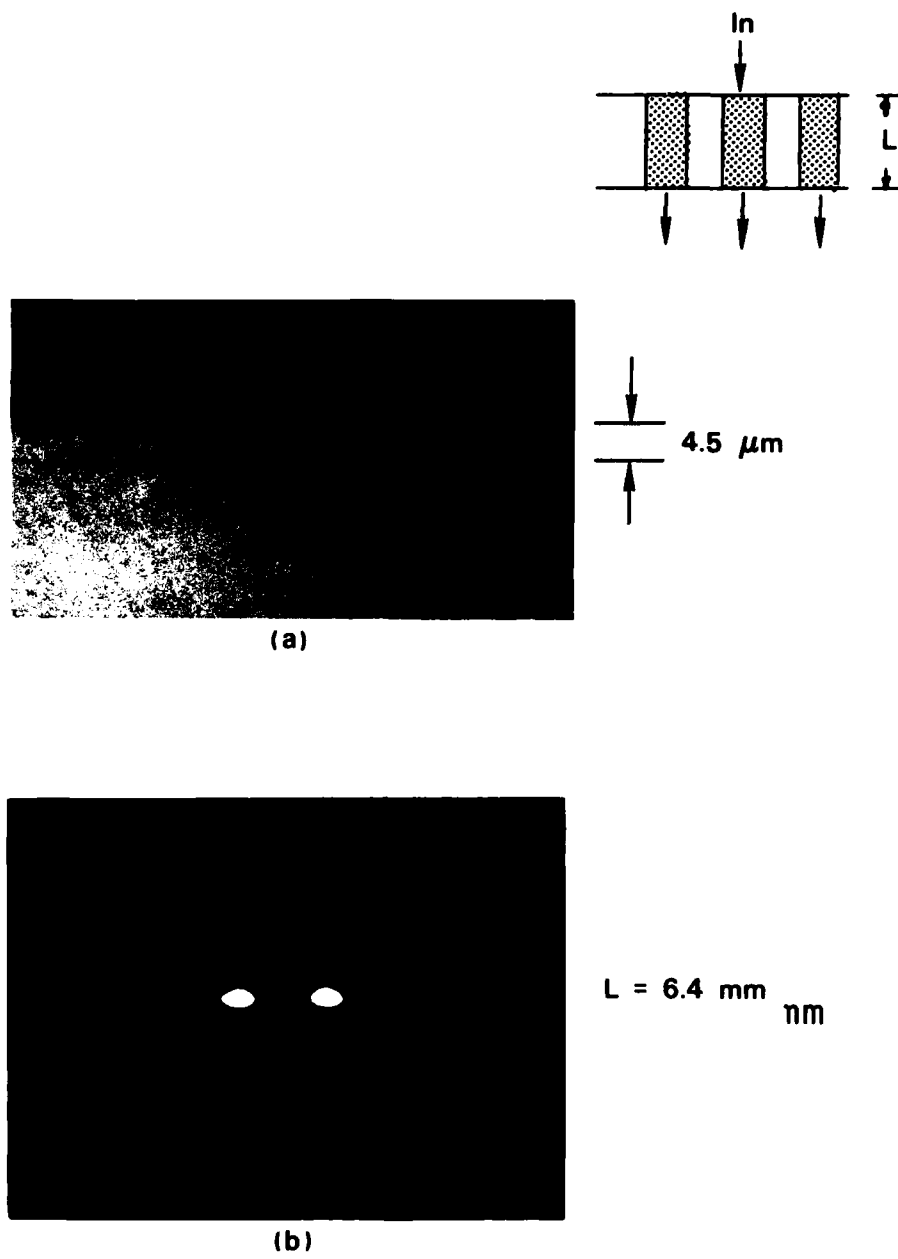


Figure 24. (a) Photomicrograph of InP oxide-confined three-guide coupler. The SiO_2 film under the guiding layer is visible. (b) Photograph of near-field output intensity pattern for light incident in the center guide; 95% of the light is coupled to the outer guides.

141721-R

field output intensity pattern. Here, 95% of the power has been transferred to the outside guides.

A phase modulator was fabricated in InP guides by Be implanting a p⁺ InP cap layer over an n-guidingh layer and then patterning the rib guides. The device is shown in Fig. 25. Au-Zn and Au-Sn alloyed contacts were used for the p and n regions, respectively. To observe intensity modulation, the device was placed between crossed polarizers with light incident at 45° to the (100) normal. The intensity vs voltage curve for the device is shown in Fig. 25. Approximately 20 V is needed to obtain a π -radian phase shift, consistent with values calculated for this structure.

IV. CONCLUSION

Q-switched semiconductor diode lasers with an integrated modulator have been studied theoretically and experimentally. Simulations show these lasers can be operated in an inversion-dumped mode of Q-switching to produce \sim 20-ps FWHM full on/off pulses with several hundred milliwatts of peak power at rates of several gigahertz for modest levels of current excitation (about twice the threshold with the modulator open-circuited). This mode of Q-switching has been verified experimentally at rates of 4 GHz. Modulation has been seen up to an instrumentation limit of 7 GHz although the depth of modulation cannot be experimentally resolved at this frequency.

Simulations and experiments also show a mode of Q-switching in which the population inversion continuously remains high. This mode of operation is capable of 20-ps pulses at rates of tens of gigahertz with a peak optical power of tens of milliwatts for modest levels of current drive.

The lasers also have considerable potential for transmitters at rates of tens of Gbit/s. While RZ PCM operation may not prove to be feasible, binary PPM appears very promising.

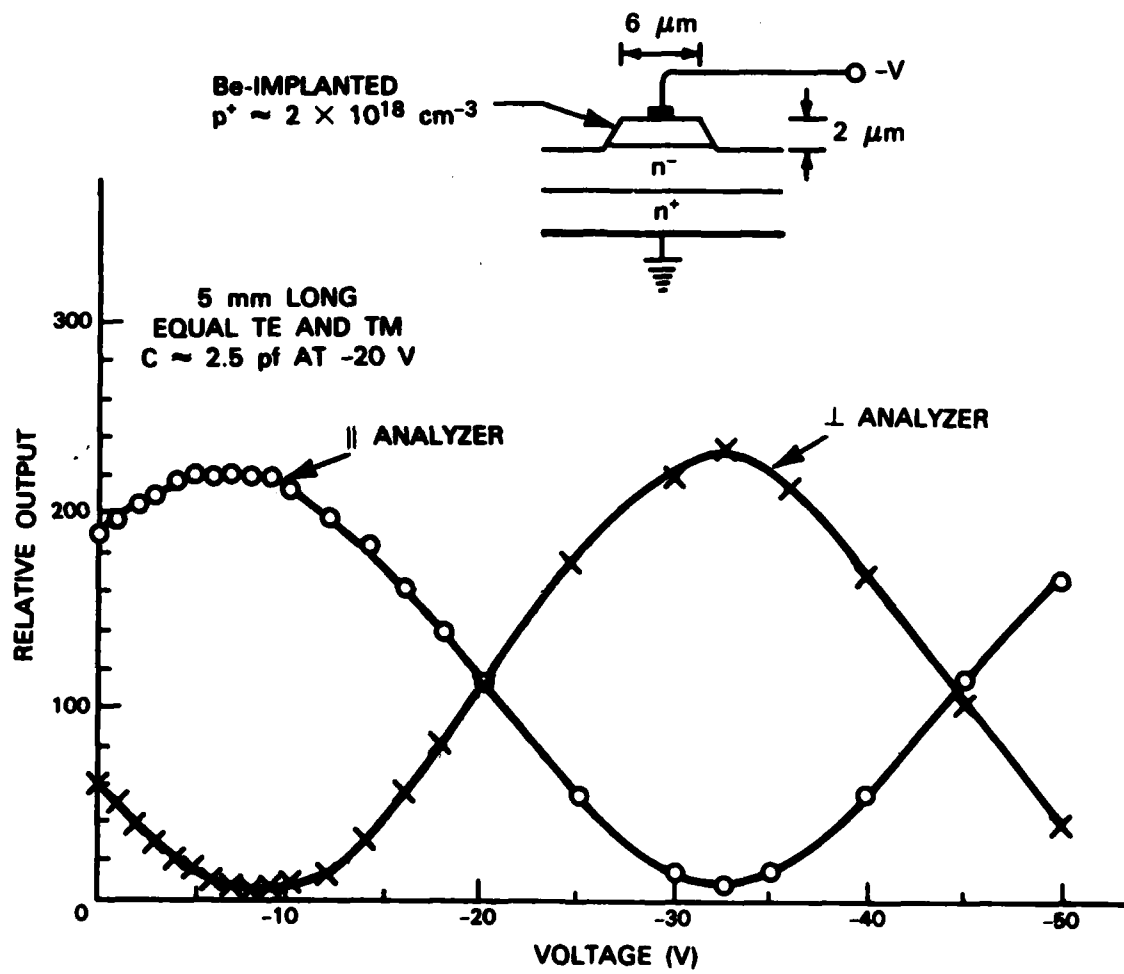


Figure 25. Output intensity vs voltage for InP pn junction rib guide modulator.

Several types of single-mode InP-based rib waveguides, three-guide couplers and phase modulators have been fabricated for use in wideband modulators. The Mach-Zehnder and special electroabsorption structures look promising for GHz analog modulation. Losses of $\approx 1.5 \text{ cm}^{-1}$ were obtained at $1.15 \mu\text{m}$ for oxide-confined guides. Initial phase modulators had a 20-V extinction voltage, and three-guide couplers had a 6-mm coupling length.

References

1. D. Z. Tsang, J. N. Walpole, S. H. Groves, J. J. Hsieh and J. P. Donnelly, *Appl. Phys. Lett.* 38, 120 (1981).
2. D. Z. Tsang and J. N. Walpole, *IEEE J. Quantum Electron.* QE-19, 145 (1983).
3. D. Z. Tsang, J. N. Walpole, Z. L. Liau and S. H. Groves, in *4th Int. Conf. Integrated Opt. Optical Fiber Commun. Postdeadline Technical Digest*, Tokyo, Japan, June 27-30, 1983, paper 2985-6.
4. Z. L. Liau and J. N. Walpole, *Appl. Phys. Lett.* 40, 568 (1982).
5. R. H. Kingston, *Appl. Phys. Lett.* 34, 744 (1979).
6. T. Tsukada and C. L. Tang, *IEEE J. Quantum Electron.*, QE-13, 37 (1977).
7. M. Yamanishi, K. Ishii, M. Ameda and T. Kawamura, *Japan. J. Appl. Phys.* 17 suppl., 359 (1978).
8. R. H. Kingston, *Appl. Phys. Lett.* 34, 744 (1979).
9. N. L. DeMeo, F. J. Leonberger and S. H. Groves, *Tech. Digest Top. Mtg. on Integ. & Guided Wave Optics*, Asilomar, CA (1982) paper WD7.
10. F. J. Leonberger, C. O. Bozler, R. W. McClelland and I. Melngailis, *Appl. Phys. Lett.* 38, 313 (1981).
11. P. Vohl, C. O. Bozler, R. W. McClelland, A. Chu and A. J. Strauss, *J. Cryst. Growth* 56, 410 (1982).
12. P. Vohl, F. J. Leonberger and F. J. O'Donnell, *Electronic Mat'l's Conf.* Santa Barbara, CA, June 1981.

UNCLASSIFIED

SECURITY CLASSIFICATION OF THIS PAGE (When Data Entered)

END

FINISHED

DNC